

# A general multiscroll Lorenz system family and its realization via digital signal processors

Simin Yu

*College of Automation, Guangdong University of Technology, Guangzhou 510090, People's Republic of China and Department of Electronic Engineering, City University of Hong Kong, Hong Kong SAR, People's Republic of China*

Jinhu Lü<sup>a)</sup>

*Key Laboratory of Systems and Control, Institute of Systems Science, Academy of Mathematics and Systems Science, Chinese Academy of Sciences, Beijing 100080, People's Republic of China and Department of Ecology and Evolutionary Biology, Princeton University, Princeton, New Jersey 08544*

Wallace K. S. Tang<sup>b)</sup> and Guanrong Chen<sup>c)</sup>

*Department of Electronic Engineering, City University of Hong Kong, Hong Kong SAR, People's Republic of China*

(Received 30 May 2006; accepted 21 July 2006; published online 13 September 2006)

This paper proposes a general multiscroll Lorenz system family by introducing a novel parameterized  $n$ th-order polynomial transformation. Some basic dynamical behaviors of this general multiscroll Lorenz system family are then investigated, including bifurcations, maximum Lyapunov exponents, and parameters regions. Furthermore, the general multiscroll Lorenz attractors are physically verified by using digital signal processors. © 2006 American Institute of Physics.

[DOI: [10.1063/1.2336739](https://doi.org/10.1063/1.2336739)]

The Lorenz system, as the first classical chaotic system, has been intensively investigated as a benchmark system for chaotic theory over the past four decades. The general Lorenz system family is a natural generalization of the classical Lorenz system, which has a similar double-scroll butterfly-like attractor. Thus, it is very interesting to ask the following questions: “Is it possible to generate various complex multiscroll chaotic attractors from the general Lorenz system family via some simple linear transformations?” “Can one implement these multiscroll chaotic attractors by using some simple physical circuits?” This paper will give positive answers to these questions. More precisely, a general multiscroll Lorenz system family is introduced by constructing a novel parameterized  $n$ th-order polynomial transformation. Then, the fundamental dynamical behaviors of this general multiscroll Lorenz system family are further explored. Finally, some novel experiments are designed via digital signal processors (DSP) to physically implement and verify these general multiscroll Lorenz attractors.

## I. INTRODUCTION

In 1963, Lorenz found the first classical chaotic system.<sup>1,2</sup> In 1999, Chen and Ueta proposed a dual system of the Lorenz system,<sup>3</sup> called Chen's system by other researchers thereafter, in the sense that the Lorenz system satisfies  $a_{12}a_{21}>0$  while the Chen system satisfies  $a_{12}a_{21}<0$  according to the classification of Vaněček and Čelikovský,<sup>4</sup> where  $a_{12}$  and  $a_{21}$  are entries in the matrix  $A=(a_{ij})_{3\times 3}$  of the linear

part of the quadratic chaotic systems. In 2002, Lü and Chen found the critical chaotic system between the Lorenz and the Chen systems, which satisfies  $a_{12}a_{21}=0$ .<sup>5–7</sup> In the same year, Lü *et al.* constructed a unified system that contains the above three related but nonequivalent chaotic systems.<sup>6,7</sup> Other than this group of generalized Lorenz systems, there are some other three-dimensional quadratic autonomous chaotic systems reported in the literature, although not directly related to the Lorenz system.<sup>8–17</sup>

Aiming for simple but nonsmooth chaotic systems, a notable one is Chua's circuit, coined in 1984, which has a double-scroll attractor. Lately, the pursuit of designing circuits to produce various multiscroll chaotic attractors became a focal subject for electronic engineers, due not only to the theoretical interest but more importantly to their potential real-world applications in various chaos-based technologies and information systems.<sup>18–30</sup> Today, there are several effective approaches available for designing multiscroll chaotic attractors, using step functions,<sup>18</sup> piecewise-linear functions,<sup>19</sup> sine functions,<sup>20</sup> switching manifolds,<sup>22,23</sup> hysteresis series,<sup>24</sup> saturated series,<sup>25,27</sup> jerk circuits,<sup>26</sup> and so on. Lü and Chen give a detailed review on the main advances in multiscroll chaos generation, including theories, methods, implementations, and applications.<sup>29</sup>

In 1993, a so-called proto-Lorenz system was formulated by Miranda and Stone based on a nonparametric quadratic polynomial transformation.<sup>30</sup> A single-scroll proto-Lorenz system, together with an  $n$ -scroll Lorenz system, were constructed. A natural question is whether all the three-dimensional quadratic autonomous chaotic systems can have similar protosystems. Another question is whether a unified algebraic form can be designed to realize them. In the fol-

<sup>a)</sup>Electronic mail: jhlu@iss.ac.cn

<sup>b)</sup>Electronic mail: kstang@ee.cityu.edu.hk

<sup>c)</sup>Electronic mail: gchen@ee.cityu.edu.hk

TABLE I. System parameters of several typical chaotic systems.

$a_1$	$a_2$	$a_{13}$	$a_{23}$	$b_1$	$b_2$	$b_{13}$	$b_{23}$	$d_2$	$c_3$	$c_{12}$	$c_{11}$	$c_{22}$	$c_{33}$	$d_3$	System
-10	10	0	0	28	-1	-1	0	0	-\$\frac{8}{3}\$	1	0	0	0	0	Lorenz
-35	35	0	0	-7	28	-1	0	0	-3	1	0	0	0	0	Chen
-36	36	0	0	0	20	-1	0	0	-3	1	0	0	0	0	Lü
2.86	0	0	-1	0	-10	1	0	1	-4	1	0	0	0	0	Lorenz-like
0.5	0	0	1	0	-10	-1	0	0	-4	-1	0	0	0	0	Liu-Chen
-2	6.7	0	-1	1	0	0	0	0	-1	0	0	1	0	0	Ruchlidge
0	1	0	0	1	-0.85	-1	0	0	-0.5	0	1	0	0	0	S-M
0	1	0	0	-1	0	0	1	0	0	0	0	-1	0	1	Sprott (I)
0	0	0	1	1	-1	0	0	0	0	-1	0	0	0	1	Sprott (II)
0	0	0	1	1	-1	0	0	0	0	0	-1	0	0	1	Sprott (III)

lowing, we give positive answers to both questions.

More precisely, this paper presents a general multiscroll Lorenz system family by introducing a novel parameterized  $n$ th-order polynomial transformation. Some typical dynamical behaviors of this new family, including bifurcations, maximum Lyapunov exponents, and parameters regions, are investigated. Moreover, the general multiscroll Lorenz attractors are physically verified by some novel experiments via digital signal processors (DSP).

The rest of the paper is organized as follows. A general multiscroll Lorenz system family is deduced in Sec. II. In Sec. III, some typical dynamical behaviors of this general multiscroll Lorenz system family are studied. A new DSP-based experimental method is described in Sec. IV for verifying the general multiscroll Lorenz chaotic attractors. Finally, conclusions are drawn in Sec. V.

## II. A GENERAL MULTISCROLL LORENZ SYSTEM FAMILY

In this section, we extend the concept of general proto-Lorenz system family,<sup>30</sup> for the design of a general multiscroll Lorenz system.

### A. A general proto-Lorenz system family

Consider the following general Lorenz system family<sup>12</sup>:

$$\begin{aligned} \frac{dx}{d\tau} &= a_1x + a_2y + a_{13}xz + a_{23}yz, \\ \frac{dy}{d\tau} &= b_1x + b_2y + b_{13}xz + b_{23}yz + d_2, \\ \frac{dz}{d\tau} &= c_3z + c_{12}xy + c_{11}x^2 + c_{22}y^2 + c_{33}z^2 + d_3, \end{aligned} \quad (1)$$

where  $a_i, b_i, a_{ij}, b_{ij}$  for  $i=1, 2$ ,  $c_{jj}$  for  $j=1, 2, 3$ , and  $c_3, d_2, d_3, c_{12}$  are real constants.

System (1) is a general form for most typical three-dimensional quadratic autonomous chaotic systems including the Lorenz system,<sup>1,2</sup> Chen system,<sup>3,7</sup> Lü system,<sup>5-7</sup> Lorenz-like system,<sup>12</sup> Liu-Chen system,<sup>13</sup> Ruchlidge system,<sup>14</sup> Shimizu-Morioka system,<sup>12</sup> and Sprott systems.<sup>15-17</sup> The parameter settings for these three-dimensional quadratic autonomous chaotic systems are tabulated in Table I.

In 1993, Miranda and Stone proposed the so-called proto-Lorenz system by introducing a nonparametric quadratic polynomial transformation on the Lorenz system.<sup>30</sup> Here, we further propose a novel parameterized quadratic polynomial transformation:

$$u = \xi_1^2 x^2 - \xi_2^2 y^2, \quad v = \xi_3 xy, \quad w = \xi_4 z, \quad (2)$$

where  $\xi_1, \xi_2, \xi_3, \xi_4$  are some control parameters. Compared with the nonparametric quadratic polynomial transformation given in Ref. 30, the above control parameters  $\xi_i$  ( $1 \leq i \leq 4$ ) can be adjusted for controlling bifurcations, maximum Lyapunov exponents, symmetry, and even the shape of the phase portraits, for different chaotic systems. These characteristics are very useful for chaos synchronization and secure communication because they greatly increase the complexity and controllability of the system, making the reconstruction of scrolls and hence attacks much more difficult.

The inverse transformation of (2) is given by

$$\begin{aligned} x^2 &= \frac{|N(u, i\xi_v v)| + u}{2\xi_1^2}, \quad y^2 = \frac{|N(u, i\xi_v v)| - u}{2\xi_2^2}, \\ xy &= \frac{v}{\xi_3}, \quad z = \frac{w}{\xi_4}, \end{aligned} \quad (3)$$

where  $\xi_v = 2\xi_1\xi_2/\xi_3$  is the control parameter,  $N(u, i\xi_v v) = u + i\xi_v v$  is the complex variable function transformation of the control parameter  $\xi_v$ , and  $|N(u, i\xi_v v)| = |u + i\xi_v v| = \sqrt{u^2 + (\xi_v v)^2}$  is the module of  $N(u, i\xi_v v)$ .

By differentiating (2), we have

$$\begin{aligned} \frac{du}{d\tau} &= 2\xi_1^2 x \frac{dx}{d\tau} - 2\xi_2^2 y \frac{dy}{d\tau}, \\ \frac{dv}{d\tau} &= \xi_3 y \frac{dx}{d\tau} + \xi_3 x \frac{dy}{d\tau}, \\ \frac{dw}{d\tau} &= \xi_4 \frac{dz}{d\tau}. \end{aligned} \quad (4)$$

Substituting (1) into (4) leads to

$$\begin{aligned} \frac{du}{d\tau} &= 2\xi_1^2(a_1x^2 + a_2xy + a_{13}x^2z + a_{23}xyz) \\ &\quad - 2\xi_2^2(b_1xy + b_2y^2 + b_{13}xyz + b_{23}y^2z + d_2y), \\ \frac{dv}{d\tau} &= \xi_3(a_1xy + a_2y^2 + a_{13}xyz + a_{23}y^2z + b_1x^2 + b_2xy \\ &\quad + b_{13}x^2z + b_{23}xyz + d_2x), \\ \frac{dw}{d\tau} &= \xi_4(c_3z + c_{12}xy + c_{11}x^2 + c_{22}y^2 + c_{33}z^2 + d_3). \end{aligned} \quad (5)$$

Further substituting (3) into (5), the general proto-Lorenz system family can be obtained, and a unified algebraic equation is formulated as below:

$$\begin{aligned} \frac{du}{d\tau} &= \left( a_1 + b_2 + \frac{(a_{13} + b_{23})w}{\xi_4} \right) u \\ &\quad + \left( \frac{2(a_2\xi_1^2 - b_1\xi_2^2)}{\xi_3} + \frac{2(a_{23}\xi_1^2 - b_{13}\xi_2^2)w}{\xi_3\xi_4} \right) v \\ &\quad + \left( a_1 - b_2 + \frac{(a_{13} - b_{23})w}{\xi_4} \right) |N(u, i\xi_v v)| \\ &\quad + \sqrt{2}d_2\xi_2\sqrt{|N(u, i\xi_v v)| - u}, \\ \frac{dv}{d\tau} &= \left( -\frac{a_2\xi_3}{2\xi_2^2} + \frac{b_1\xi_3}{2\xi_1^2} - \frac{a_{23}\xi_3w}{2\xi_2\xi_4} + \frac{b_{13}\xi_3w}{2\xi_1\xi_4} \right) u \\ &\quad + \left( a_1 + b_2 + \frac{(a_{13} + b_{23})w}{\xi_4} \right) v \\ &\quad + \left( \frac{a_2\xi_3}{2\xi_2^2} + \frac{b_1\xi_3}{2\xi_1^2} + \frac{a_{23}\xi_3w}{2\xi_2\xi_4} + \frac{b_{13}\xi_3w}{2\xi_1\xi_4} \right) |N(u, i\xi_v v)| \end{aligned}$$

$$- \frac{d_2\xi_3}{\sqrt{2}\xi_1}\sqrt{|N(u, i\xi_v v)| + u}, \quad (6)$$

$$\begin{aligned} \frac{dw}{d\tau} &= \left( \frac{c_{11}\xi_4}{2\xi_1^2} - \frac{c_{22}\xi_4}{2\xi_2^2} \right) u + \frac{c_{12}\xi_4}{\xi_3} v \\ &\quad + \left( \frac{c_{11}\xi_4}{2\xi_1^2} + \frac{c_{22}\xi_4}{2\xi_2^2} \right) |N(u, i\xi_v v)| \\ &\quad + \left( \frac{c_{33}}{\xi_4}w^2 + c_3w + d_3\xi_4 \right). \end{aligned}$$

According to Table I and system (6), one can obtain the explicit expressions of various single-scroll protosystems, such as proto-Lorenz, proto-Chen, and proto-Lü systems, while the complex variable function  $N(u, i\xi_v v) = u + i\xi_v v$  plays a key role in the dynamics of the general system (6).

## B. A general multiscroll Lorenz system family

Based on the general single-scroll proto-Lorenz system family expressed in (6), a general multiscroll Lorenz system family can be designed by means of a novel  $n$ th-order polynomial transformation.

Recall  $N(u, i\xi_v v) = u + i\xi_v v$ , an  $n$ th-order polynomial can be expressed as follows:

$$[N(p, i\xi_q q)]^n = (p + i\xi_q q)^n, \quad (7)$$

where  $\xi_q = \xi_v$  is a control parameter. The corresponding  $n$ th-order conjugate polynomial is given by

$$[\tilde{N}(p, i\xi_q q)]^n = (p - i\xi_q q)^n. \quad (8)$$

The real and imaginary parts of the  $n$ th-order polynomial  $[N(p, i\xi_q q)]^n$  can be described, respectively, by

$$P_n(p, \xi_q q) = \text{Re}\{[N(p, i\xi_q q)]^n\} = \begin{cases} p^n + \sum_{l=1}^{n/2} (-1)^l \frac{\prod_{j=0}^{2l-1} (n-j)}{(2l)!} p^{n-2l} (\xi_q q)^{2l}, & n \text{ is even} \\ p^n + \sum_{l=1}^{(n-1)/2} (-1)^l \frac{\prod_{j=0}^{2l-1} (n-j)}{(2l)!} p^{n-2l} (\xi_q q)^{2l}, & n \text{ is odd} \end{cases} \quad (9)$$

and

$$Q_n(p, \xi_q q) = \text{Im}\{[N(p, i\xi_q q)]^n\} = \begin{cases} \sum_{l=1}^{n/2} (-1)^{l+1} \frac{\prod_{j=0}^{2l-2} (n-j)}{(2l-1)!} p^{n-2l+1} (\xi_q q)^{2l-1}, & n \text{ is even} \\ \sum_{l=1}^{(n+1)/2} (-1)^{l+1} \frac{\prod_{j=0}^{2l-2} (n-j)}{(2l-1)!} p^{n-2l+1} (\xi_q q)^{2l-1}, & n \text{ is odd}. \end{cases} \quad (10)$$

Similarly, the real and imaginary parts of the  $(n-1)$ st-order polynomial  $[\tilde{N}(p, i\xi_q q)]^{n-1}$  are described respectively by

$$\tilde{P}_{n-1}(p, \xi_q q) = \text{Re}\{[\tilde{N}(p, i\xi_q q)]^{n-1}\} = \begin{cases} p^{n-1} + \sum_{l=1}^{(n-2)/2} (-1)^l \frac{\prod_{j=0}^{2l-1} (n-j-1)}{(2l)!} p^{n-2l-1} (\xi_q q)^{2l}, & n \text{ is even} \\ p^{n-1} + \sum_{l=1}^{(n-1)/2} (-1)^l \frac{\prod_{j=0}^{2l-1} (n-j-1)}{(2l)!} p^{n-2l-1} (\xi_q q)^{2l}, & n \text{ is odd} \end{cases} \quad (11)$$

and

$$\tilde{Q}_{n-1}(p, \xi_q q) = \text{Im}\{\tilde{N}(p, i\xi_q q)\}^{n-1} = \begin{cases} \sum_{l=1}^{n/2} (-1)^l \frac{\prod_{j=0}^{2l-2} (n-j-1)}{(2l-1)!} p^{n-2l} (\xi_q q)^{2l-1}, & n \text{ is even} \\ \sum_{l=1}^{(n-1)/2} (-1)^l \frac{\prod_{j=0}^{2l-2} (n-j-1)}{(2l-1)!} p^{n-2l} (\xi_q q)^{2l-1}, & n \text{ is odd.} \end{cases} \quad (12)$$

According to the general single-scroll proto-Lorenz system family (6), the  $n$ th-order polynomial  $[N(p, i\xi_q q)]^n$  and  $(n-1)$ th-order polynomial  $[\tilde{N}(p, i\xi_q q)]^{n-1}$ , after some tedious algebraic manipulations, a unified system equation for the general multiscroll Lorenz system family is obtained as below:

$$\begin{pmatrix} \frac{dp}{d\tau} \\ \frac{dq}{d\tau} \\ \frac{ds}{d\tau} \end{pmatrix} = \begin{pmatrix} \frac{\tilde{P}_{n-1}(p, \xi_q q)}{n|N(p, i\xi_q q)|^{2n-2}} & -\frac{\tilde{Q}_{n-1}(p, \xi_q q)}{n|N(p, i\xi_q q)|^{2n-2}} & 0 \\ \frac{\tilde{Q}_{n-1}(p, \xi_q q)}{n|N(p, i\xi_q q)|^{2n-2}} & \frac{\tilde{P}_{n-1}(p, \xi_q q)}{n|N(p, i\xi_q q)|^{2n-2}} & 0 \\ 0 & 0 & 1 \end{pmatrix} \times \begin{pmatrix} F_1(p, q, s, \xi) \\ F_2(p, q, s, \xi) \\ F_3(p, q, s, \xi) \end{pmatrix}, \quad (13)$$

where  $s=w$ ,  $n|N(p, i\xi_q q)|^{2n-2}=n[p^2+(\xi_q q)^2]^{n-1}$ ,  $\tilde{P}_{n-1}(p, \xi_q q)$ , and  $\tilde{Q}_{n-1}(p, \xi_q q)$  are the real and imaginary parts of the  $(n-1)$ th-order polynomial  $[\tilde{N}(p, i\xi_q q)]^{n-1}$  given by (11) and (12), respectively.

By replacing  $u, v, w, |N(u, i\xi_v v)|$  in (6) with  $P_n(p, \xi_q q), Q_n(p, \xi_q q), s, |N(u, i\xi_v v)|^{n/2}$ , respectively, the following explicit mathematical expressions of  $F_1(p, q, s, \xi), F_2(p, q, s, \xi), F_3(p, q, s, \xi)$  can be obtained:

$$\begin{aligned} F_1(p, q, s, \xi) &= \left( a_1 + b_2 + \frac{(a_{13} + b_{23})s}{\xi_4} \right) P_n(p, \xi_q q) \\ &\quad + \left( \frac{2(a_2 \xi_1^2 - b_1 \xi_2^2)}{\xi_3} \right. \\ &\quad \left. + \frac{2(a_{23} \xi_1^2 - b_{13} \xi_2^2)s}{\xi_3 \xi_4} \right) Q_n(p, \xi_q q) \\ &\quad + \left( a_1 - b_2 + \frac{(a_{13} - b_{23})s}{\xi_4} \right) |N(p, i\xi_q q)|^{n/2} \\ &\quad + \sqrt{2} d_2 \xi_2 \sqrt{|N(p, i\xi_q q)|^{n/2} - p}, \end{aligned}$$

$$\begin{aligned} F_2(p, q, s, \xi) &= \left( -\frac{a_2 \xi_3}{2 \xi_2} + \frac{b_1 \xi_3}{2 \xi_1} - \frac{a_{23} \xi_3 s}{2 \xi_2^2 \xi_4} + \frac{b_{13} \xi_3 s}{2 \xi_1^2 \xi_4} \right) P_n(p, \xi_q q) \\ &\quad + \left( a_1 + b_2 + \frac{(a_{13} + b_{23})s}{\xi_4} \right) Q_n(p, \xi_q q) \\ &\quad + \left( \frac{a_2 \xi_3}{2 \xi_2^2} + \frac{b_1 \xi_3}{2 \xi_1^2} + \frac{a_{23} \xi_3 s}{2 \xi_2^2 \xi_4} + \frac{b_{13} \xi_3 s}{2 \xi_1^2 \xi_4} \right) \end{aligned}$$

$$\times |N(p, i\xi_q q)|^{n/2} - \frac{d_2 \xi_3}{\sqrt{2} \xi_1} \sqrt{|N(p, i\xi_q q)|^{n/2} + p}, \quad (14)$$

$$\begin{aligned} F_3(p, q, s, \xi) &= \left( \frac{c_{11} \xi_4}{2 \xi_1^2} - \frac{c_{22} \xi_4}{2 \xi_2^2} \right) P_n(p, \xi_q q) + \frac{c_{12} \xi_4}{\xi_3} Q_n(p, \xi_q q) \\ &\quad + \left( \frac{c_{11} \xi_4}{2 \xi_1^2} + \frac{c_{22} \xi_4}{2 \xi_2^2} \right) |N(p, i\xi_q q)|^{n/2} \\ &\quad + \left( \frac{c_{33}}{\xi_4} s^2 + c_3 s + d_3 \xi_4 \right), \end{aligned}$$

where  $\xi = (\xi_1, \xi_2, \xi_3, \xi_4, \xi_q)$ .

### III. DYNAMICAL BEHAVIORS OF THE GENERAL MULTISCROLL LORENZ SYSTEM FAMILY

Rewrite (13) in the following form:

$$\begin{aligned} \frac{dp}{d\tau} &= \frac{\tilde{P}_{n-1}(p, \xi_q q)}{n|N(p, i\xi_q q)|^{2n-2}} F_1(p, q, s, \xi) \\ &\quad - \frac{\tilde{Q}_{n-1}(p, \xi_q q)}{n|N(p, i\xi_q q)|^{2n-2}} F_2(p, q, s, \xi), \\ \frac{dq}{d\tau} &= \frac{\tilde{Q}_{n-1}(p, \xi_q q)}{n|N(p, i\xi_q q)|^{2n-2}} F_1(p, q, s, \xi) \\ &\quad + \frac{\tilde{P}_{n-1}(p, \xi_q q)}{n|N(p, i\xi_q q)|^{2n-2}} F_2(p, q, s, \xi), \quad (15) \\ \frac{ds}{d\tau} &= \left( \frac{c_{11} \xi_4}{2 \xi_1^2} - \frac{c_{22} \xi_4}{2 \xi_2^2} \right) P_n(p, \xi_q q) + \frac{c_{12} \xi_4}{\xi_3} Q_n(p, \xi_q q) \\ &\quad + \left( \frac{c_{11} \xi_4}{2 \xi_1^2} + \frac{c_{22} \xi_4}{2 \xi_2^2} \right) |N(p, i\xi_q q)|^{n/2} \\ &\quad + \left( \frac{c_{33}}{\xi_4} s^2 + c_3 s + d_3 \xi_4 \right). \end{aligned}$$

The dynamical behaviors of the general multiscroll Lorenz system family (15), including bifurcations, maximum Lyapunov exponents, and parameters regions, are studied.

#### A. Basic dynamical behaviors

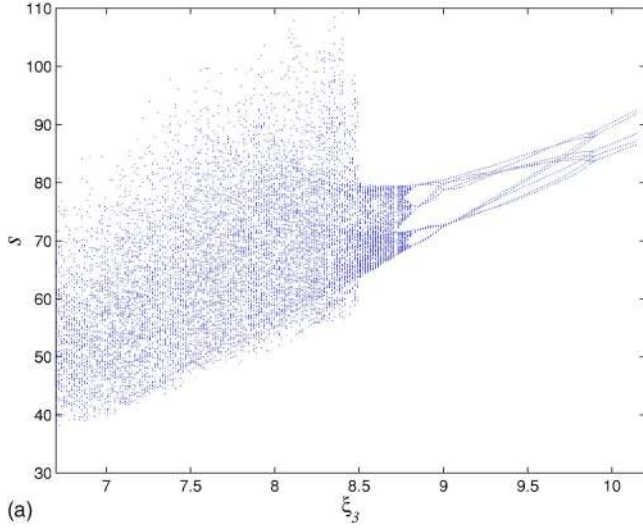
For brevity, only a ten-scroll Lü system is used as an example for explaining our methodology. The similar procedures are also applicable for all the other cases.

From Table I and Eqs. (9)–(15) with  $n=10$ , the ten-scroll Lü system is described by

$$\begin{aligned} \frac{dp}{d\tau} &= \frac{\tilde{P}_9(p, \xi_q q)}{10 \times [p^2 + (\xi_q q)^2]^9} F_1(p, q, s, \xi) \\ &\quad - \frac{\tilde{Q}_9(p, \xi_q q)}{10 \times [p^2 + (\xi_q q)^2]^9} F_2(p, q, s, \xi), \\ \frac{dq}{d\tau} &= \frac{\tilde{Q}_9(p, \xi_q q)}{10 \times [p^2 + (\xi_q q)^2]^9} F_1(p, q, s, \xi) \\ &\quad + \frac{\tilde{P}_9(p, \xi_q q)}{10 \times [p^2 + (\xi_q q)^2]^9} F_2(p, q, s, \xi), \end{aligned} \quad (16)$$

$$\frac{ds}{d\tau} = \frac{\xi_4}{\xi_3} Q_{10}(p, \xi_q q) - 3s.$$

Based on Eqs. (9)–(12) and (14), the mathematical expressions of  $\tilde{P}_9(p, \xi_q q)$ ,  $\tilde{Q}_9(p, \xi_q q)$ ,  $P_{10}(p, \xi_q q)$ ,  $Q_{10}(p, \xi_q q)$ ,  $F_1(p, q, s, \xi)$ ,  $F_2(p, q, s, \xi)$  are obtained as



(a)

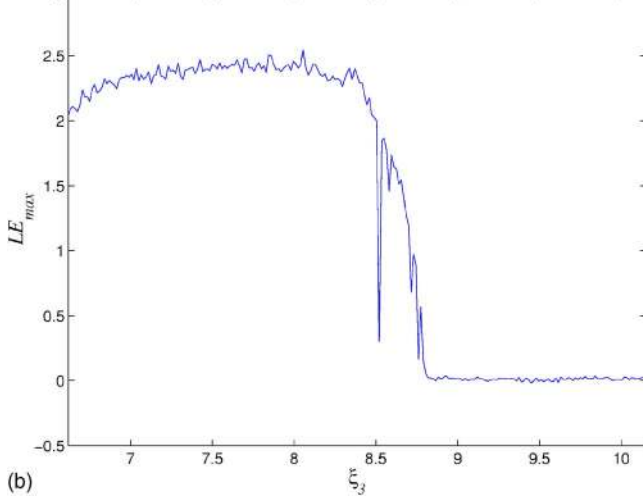
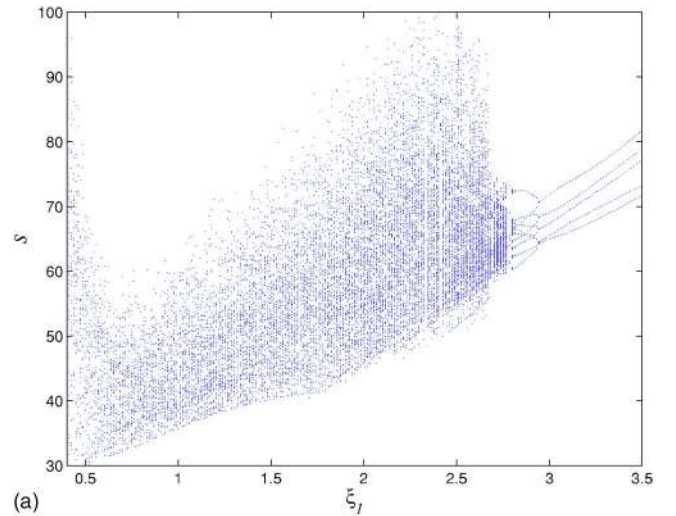


FIG. 1. Dynamical behaviors of system (16) in case I. (a) Bifurcation diagram and (b) maximum Lyapunov exponent spectrum.

$$\begin{aligned} \tilde{P}_9(p, \xi_q q) &= p^9 - 36p^7(\xi_q q)^2 + 126p^5(\xi_q q)^4 - 84p^3(\xi_q q)^6 \\ &\quad + 9p(\xi_q q)^8, \\ \tilde{Q}_9(p, \xi_q q) &= -9p^8\xi_q q + 84p^6(\xi_q q)^3 - 126p^5(\xi_q q)^4 \\ &\quad + 36p^2(\xi_q q)^7 - (\xi_q q)^9, \\ P_{10}(p, \xi_q q) &= p^{10} - 45p^8(\xi_q q)^2 + 210p^6(\xi_q q)^4 \\ &\quad - 210p^4(\xi_q q)^6 + 45p^2(\xi_q q)^8 - (\xi_q q)^{10}, \\ Q_{10}(p, \xi_q q) &= 10p^9\xi_q q - 120p^7(\xi_q q)^3 + 252p^5(\xi_q q)^5 \\ &\quad - 120p^3(\xi_q q)^7 + 10p(\xi_q q)^9 \end{aligned} \quad (17)$$

and

$$\begin{aligned} F_1(p, q, s, \xi) &= -14P_{10}(p, \xi_q q) \\ &\quad + \left( \frac{72\xi_1^2}{\xi_3} + \frac{2\xi_2^2 s}{\xi_3 \xi_4} \right) Q_{10}(p, \xi_q q) \\ &\quad + 58[p^2 + (\xi_q q)^2]^5, \end{aligned}$$



(a)

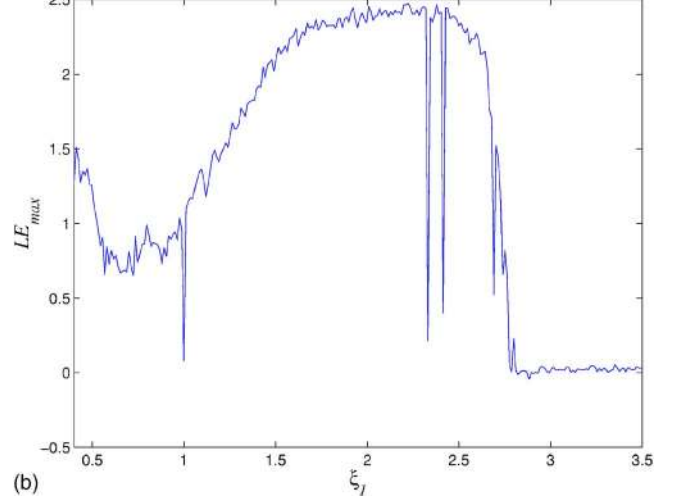


FIG. 2. Dynamical behaviors of system (16) in case II. (a) Bifurcation diagram and (b) maximum Lyapunov exponent spectrum.

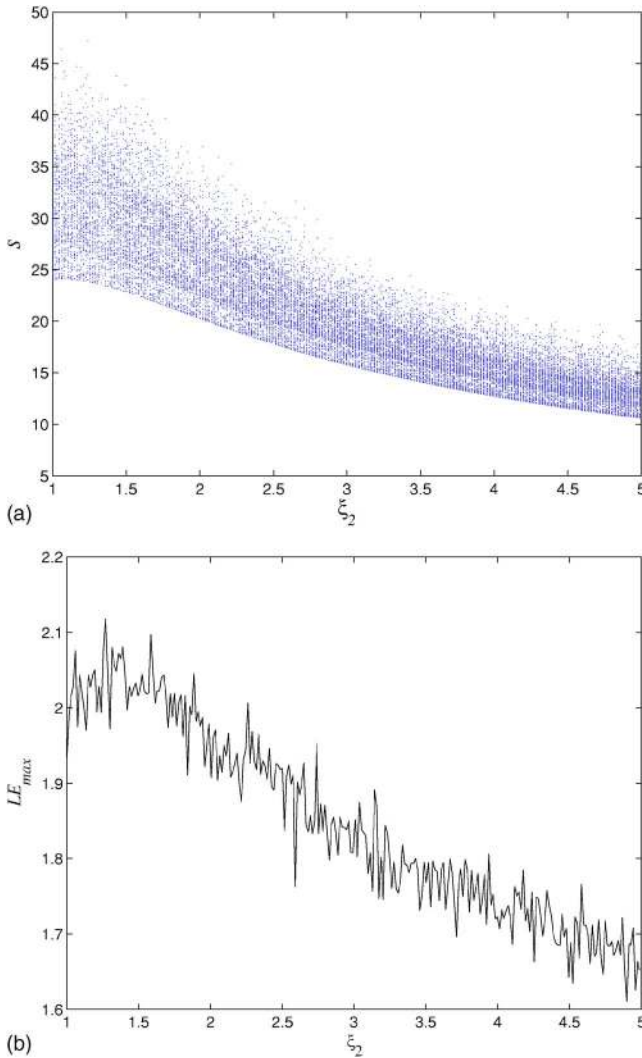


FIG. 3. Dynamical behaviors of system (16) in case III. (a) Bifurcation diagram and (b) maximum Lyapunov exponent spectrum.

$$\begin{aligned}
 F_2(p, q, s, \xi) = & \left( -\frac{36\xi_3}{2\xi_2^2} - \frac{\xi_3 s}{2\xi_1\xi_4} \right) P_{10}(p, \xi_q q) \\
 & - 14Q_{10}(p, \xi_q q) \\
 & + \left( \frac{36\xi_3}{2\xi_2^2} - \frac{\xi_3 s}{2\xi_1\xi_4} \right) [p^2 + (\xi_q q)^2]^5. \quad (18)
 \end{aligned}$$

TABLE III. Typical control parameter sets of the general multiscroll Lorenz system family (15).

$\xi_1$	$\xi_2$	$\mu$	$\xi_3$	$\xi_4$	$\xi_q$	System
3	3	2.0	18.0	3	1.00	Lorenz
4	4	2.0	32.0	5	1.00	Chen
1	5	1.7	8.5	2	1.18	Lü
5	5	1.5	37.5	2	1.00	Lorenz-like
5	5	2.0	50.0	2	1.00	Liu-Chen
3	3	2.2	19.8	2	0.91	Ruchlidge
4	4	2.3	36.8	2	0.87	S-M
1	1	2.0	2.0	2	1.00	Sprott (I)
2	2	2.0	8.0	3	1.00	Sprott (II)
1	1	2.0	2.0	1	1.00	Sprott (III)

Therefore, system (16) is completely determined by the control parameter vector  $\xi = (\xi_1, \xi_2, \xi_3, \xi_4, \xi_q)$ . Hereafter,  $\mu = \xi_3 / (\xi_1 \xi_2)$ .

The dynamical behaviors of system (16) are now further discussed, under the following three sets of control parameters:

Case I: Let  $\xi_1 = \xi_2 = 2.1$ ,  $\xi_3 = 1.5 \xi_1 \xi_2 \sim 2.3$ ,  $\xi_4 = 6.615 \sim 10.143$ ,  $\xi_q = 2 \xi_1 \xi_2 / \xi_3$ . Figures 1(a) and 1(b) show the bifurcation diagram and maximum Lyapunov exponents of system (16) versus the control parameter  $\xi_3$ .

Case II: Let  $\xi_1 = \xi_2 = 0.4 \sim 3.5$ ,  $\xi_3 = 1.7 \xi_1 \xi_2$ ,  $\xi_4 = 2$ ,  $\xi_q = 2 \xi_1 \xi_2 / \xi_3$ . Figures 2(a) and 2(b) show the bifurcation diagram and maximum Lyapunov exponents of system (16) versus the control parameter  $\xi_1$ .

Case III: Let  $\xi_1 = 1$ ,  $\xi_2 = 1 \sim 5$ ,  $\xi_3 = 2 \xi_1 \xi_2$ ,  $\xi_4 = 1$ ,  $\xi_q = 2 \xi_1 \xi_2 / \xi_3$ . Figures 3(a) and 3(b) show the bifurcation diagram and maximum Lyapunov exponents of system (16) versus the control parameter  $\xi_2$ .

It can be seen from Figs. 1–3 that there exists the typical route from period-doubling bifurcations to chaos in some given parameter regions with the positive maximum Lyapunov exponents.

Table II shows the regions of the control parameters of the general multiscroll Lorenz system family (15). According to Table II, the regions of control parameter  $\xi_3$  are completely determined by the control parameters  $\xi_1, \xi_2$ . Moreover, the magnitude of variable  $s$  is determined by the con-

TABLE II. Regions of the control parameters of the general multiscroll Lorenz system family (15).

$\xi_1$	$\xi_2$	Region	$\mu$	$\xi_3$	$\xi_4$	$\xi_q = 2 \xi_1 \xi_2 / \xi_3$	System
1~5	1~5	$\xi_2 \leq \xi_1 \leq 5$	2.0~2.5	$\xi_3 = \mu \xi_1 \xi_2$	1~5	0.8~1.0	Lorenz
1~6	1~6	$\xi_1 = \xi_2$	1.6~2.5	$\xi_3 = \mu \xi_1 \xi_2$	1~5	0.8~1.25	Chen
1~3	1~5	$\xi_1 \leq \xi_2 \leq 5$	1.5~2.3	$\xi_3 = \mu \xi_1 \xi_2$	1~5	0.87~1.33	Lü
1~6	1~6	$\xi_1 = \xi_2$	1.5~2.4	$\xi_3 = \mu \xi_1 \xi_2$	1~6	0.83~1.33	Lorenz-like
1~6	1~6	$\xi_1 = \xi_2$	2.0	$\xi_3 = \mu \xi_1 \xi_2$	1~6	1.0	Liu-Chen
1~6	1~6	$\xi_1 = \xi_2$	1.8~2.2	$\xi_3 = \mu \xi_1 \xi_2$	1~6	0.91~1.11	Ruchlidge
1~6	1~6	$\xi_1 = \xi_2$	2.0~2.3	$\xi_3 = \mu \xi_1 \xi_2$	1~6	0.87~1.0	S-M
1~6	1~6	$\xi_1 = \xi_2$	2.0	$\xi_3 = \mu \xi_1 \xi_2$	1~3	1.0	Sprott (I)
1~6	1~6	$\xi_1 = \xi_2$	2.0	$\xi_3 = \mu \xi_1 \xi_2$	1~3	1.0	Sprott (II)
1~6	1~6	$\xi_1 = \xi_2$	2.0	$\xi_3 = \mu \xi_1 \xi_2$	1~3	1.0	Sprott (III)

trol parameter  $\xi_4$ . Furthermore, the parameter  $\mu=\xi_3/(\xi_1\xi_2)$  can control the symmetry, the shape of phase portraits, and the number of scrolls of the multiscroll system family (15). For example, when  $\mu=2.0$ , the scrolls are arranged in a circle; however, when  $\mu\neq 2.0$ , the scrolls are arranged in an ellipse. Such design flexibility has greatly enhanced the potential application of this kind of system in secure communications, as the complexity of the dynamics can be well designed or increased.

## B. Numerical simulations

A number of simulations have been carried out to verify our design. The ten sets of typical control parameters in the general multiscroll Lorenz system family are given in Table III. With Eqs. (14) and (15) and Tables I and III, the general ten-scroll Lorenz chaotic attractors, including a ten-scroll Lorenz attractor, a ten-scroll Chen attractor, a ten-scroll Lü attractor, a ten-scroll Lorenz-like attractor, a ten-scroll Liu-Chen attractor, a ten-scroll Ruchlidge attractor, a ten-scroll S-M attractor, and some ten-scroll Sprott attractors, are obtained as shown in Fig. 4.

## IV. DSP-BASED EXPERIMENTS ON THE GENERAL MULTISCROLL LORENZ SYSTEM FAMILY

According to (13) [or (15)], the general multiscroll Lorenz system family has very complex algebraic form. In general, an  $n$ -scroll system is a rational fraction with the maximal power of  $(2n-2)$ . For example, the ten-scroll system (16) is a rational fraction with the maximal power of 18. In addition, some complex algebraic operations in (13), such as division and extraction, are also involved. Therefore, it is very difficult (even impossible) to implement system (13)

with large number of scrolls by using the conventional analog circuits. However, DSP-based experiments can overcome these difficulties and easily implement system (13). It also provides a basis for the future real-world applications of the general multiscroll Lorenz system family.

In our experiments, the Texas Instrument DSP device TMS320F2812 is employed. TMS320F2812 is a 32-bit DSP running at 150 MHz with fixed point operations. Such a high-speed clock rate is considered to be sufficient for our laboratory experiments. It can easily interface with external devices, such as multichannels digital-to-analog converter (DAC), which is useful for displaying the states of the realized chaotic systems, or communicated with personal computers for the ease of software development and debugging.

In order to realize the general multiscroll Lorenz system family (15), two major steps are involved. First, the continuous-time system (15) is discretized. This can be done by approximating the differentiation with difference, i.e.,

$$\frac{du}{dt} = \frac{U(m) - U(m-1)}{\Delta T},$$

where  $\Delta T$  is the sampling period. Second, rescaling of the system variables is required in order to increase the computational precision. From Fig. 4, it can be observed that the ranges of variables  $p, q$  are very small ( $|p|, |q| < 3$ ), and hence a direct implementation will affect the computational precision. For this reason, a scaling factor  $E > 1$  (in our experiment,  $E = 10$ ) is adopted.

Discretizing (15) and letting  $f = Ep$ ,  $g = Eq$ ,  $h = Es$ , the difference equations for  $f(m)$ ,  $g(m)$ ,  $h(m)$  are obtained as follows:

$$f(m) = \Delta T \cdot E \left\{ \frac{\tilde{P}_{n-1}\left(\frac{f(m-1)}{E}, \xi_q \frac{g(m-1)}{E}\right)}{n \left| N\left(\frac{f(m-1)}{E}, i\xi_q \frac{g(m-1)}{E}\right) \right|^{2n-2}} \cdot F_1\left(\frac{f(m-1)}{E}, \frac{g(m-1)}{E}, \frac{h(m-1)}{E}, \xi\right) \right. \\ \left. - \frac{\tilde{Q}_{n-1}\left(\frac{f(m-1)}{E}, \xi_q \frac{g(m-1)}{E}\right)}{n \left| N\left(\frac{f(m-1)}{E}, i\xi_q \frac{g(m-1)}{E}\right) \right|^{2n-2}} \cdot F_2\left(\frac{f(m-1)}{E}, \frac{g(m-1)}{E}, \frac{h(m-1)}{E}, \xi\right) \right\} + f(m-1), \quad (19)$$

$$g(m) = \Delta T \cdot E \left\{ \frac{\tilde{Q}_{n-1}\left(\frac{f(m-1)}{E}, \xi_q \frac{g(m-1)}{E}\right)}{n \left| N\left(\frac{f(m-1)}{E}, i\xi_q \frac{g(m-1)}{E}\right) \right|^{2n-2}} \cdot F_1\left(\frac{f(m-1)}{E}, \frac{g(m-1)}{E}, \frac{h(m-1)}{E}, \xi\right) \right. \\ \left. + \frac{\tilde{P}_{n-1}\left(\frac{f(m-1)}{E}, \xi_q \frac{g(m-1)}{E}\right)}{n \left| N\left(\frac{f(m-1)}{E}, i\xi_q \frac{g(m-1)}{E}\right) \right|^{2n-2}} \cdot F_2\left(\frac{f(m-1)}{E}, \frac{g(m-1)}{E}, \frac{h(m-1)}{E}, \xi\right) + g(m-1), \right\} + g(m-1), \quad (20)$$

and

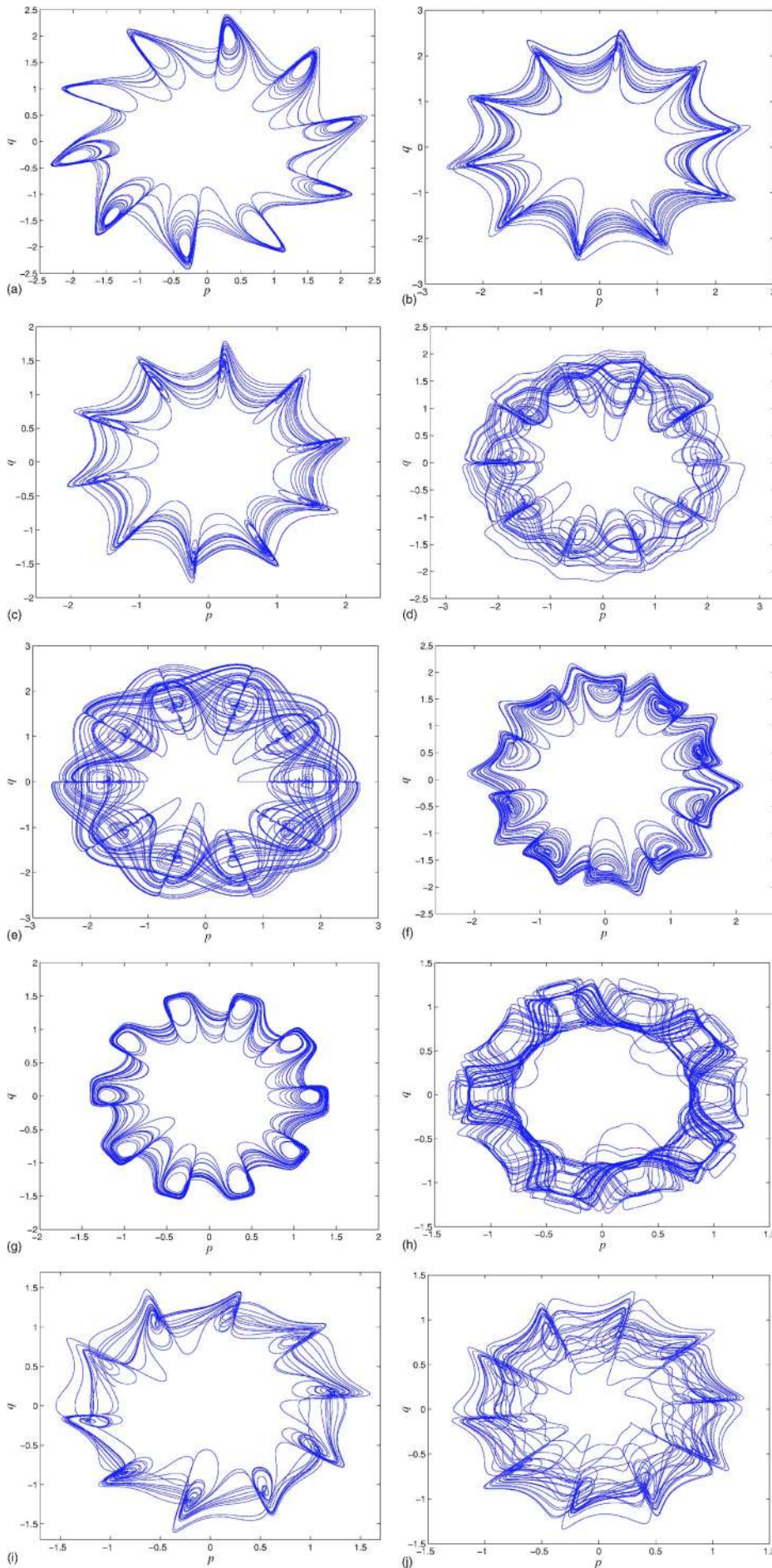


FIG. 4. Attractors of the general multiscroll Lorenz system family. (a) Ten-scroll Lorenz attractor; (b) ten-scroll Chen attractor; (c) ten-scroll Lü attractor; (d) ten-scroll Lorenz-like attractor; (e) ten-scroll Liu attractor; (f) ten-scroll Ruchlidge attractor; (g) ten-scroll S-M attractor; (h) ten-scroll Sprott attractor (I); (i) ten-scroll Sprott attractor (II); and (j) ten-scroll Sprott attractor (III).

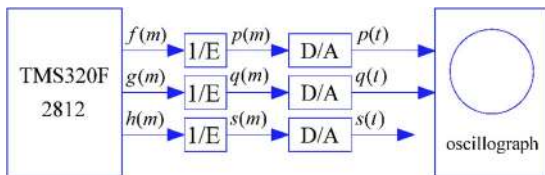


FIG. 5. Diagram of DSP working principle for realizing the general multiscroll Lorenz attractors.

$$\begin{aligned}
 h(m) = & \Delta T \cdot E \left\{ \left( \frac{c_{11}\xi_4}{2\xi_1^2} - \frac{c_{22}\xi_4}{2\xi_2^2} \right) \cdot P_n \left( \frac{f(m-1)}{E}, \xi_q \frac{g(m-1)}{E} \right) \right. \\
 & + \frac{c_{12}\xi_4}{\xi_3} \cdot Q_n \left( \frac{f(m-1)}{E}, \xi_q \frac{g(m-1)}{E} \right) \\
 & + \left( \frac{c_{11}\xi_4}{2\xi_1^2} + \frac{c_{22}\xi_4}{2\xi_2^2} \right) \cdot \left| N \left( \frac{f(m-1)}{E}, i\xi_q \frac{g(m-1)}{E} \right) \right|^{n/2} \\
 & + \left( \frac{c_{33}}{\xi_4} \left( \frac{h(m-1)}{E} \right)^2 + c_3 \frac{h(m-1)}{E} + d_3 \xi_4 \right) \Big\} \\
 & + h(m-1).
 \end{aligned} \quad (21)$$

in which the system parameters are given in Table III.

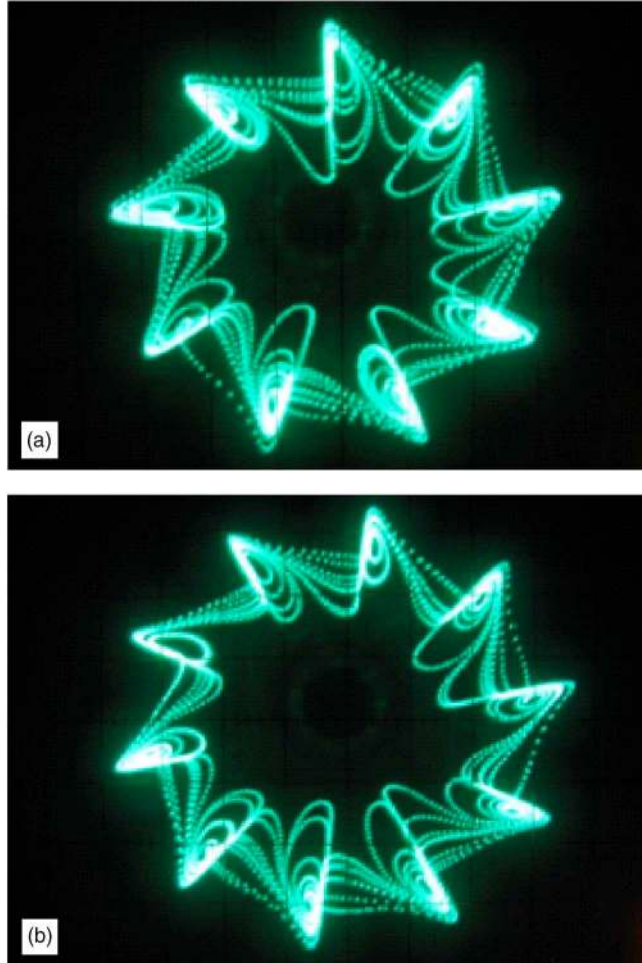


FIG. 6. Multiscroll Lorenz attractors, where  $p=q=0.7$  V/div. (a) Nine scroll and (b) ten scroll.

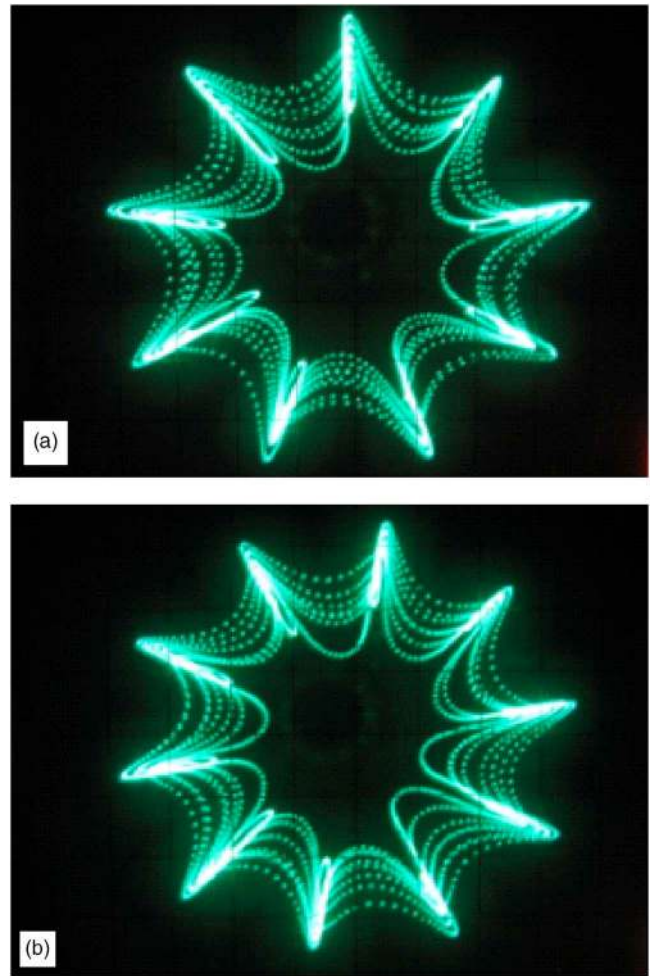


FIG. 7. Multiscroll Chen attractors, where  $p=q=0.7$  V/div. (a) Nine scroll and (b) ten scroll.

The sampling period,  $\Delta T$ , is determined by the original chaotic equation, which is usually varied with different chaotic systems. For example,  $\Delta T$  is selected as 0.015 for the multiscroll Lorenz system while 0.005 is used for Chen system.

Figure 5 shows the basic diagram of working principle, and the operational procedures are listed as follows: (1) generating the discrete-time sequence  $f(m)$ ,  $g(m)$ ,  $h(m)$  ( $m = 1, 2, \dots$ ) from (19)–(21) with some initial values of  $f(0)$ ,  $g(0)$ , and  $h(0)$ . In our experiments, they are arbitrarily set as  $f(0)=0.01$ ,  $g(0)=0.01$ ,  $h(0)=0.03$ ; (2) obtaining the discrete-time sequence of  $p$ ,  $q$  and  $s$ , by computing  $p(m) = f(m)/E$ ,  $q(m) = g(m)/E$ ,  $s(m) = h(m)/E$ ; (3) converting the digital signals  $p(m)$ ,  $q(m)$ ,  $s(m)$  to the analog signals  $p(t)$ ,  $q(t)$ ,  $s(t)$  using the multichannel DAC.

Figures 6 and 7 show the experimental observations of the nine- and ten-scroll Lorenz attractors and Chen attractors, respectively. It is also experimentally found that the use of DSP can improve the robustness against the variations of system parameters, the sampling time  $\Delta T$ , and the scaling factor  $E$ .

## V. CONCLUSIONS

In this paper, a general multiscroll Lorenz system family has been developed by constructing a novel parameterized

*n*th-order polynomial transformation. Some typical dynamical behaviors of this new chaotic family, including bifurcations, maximum Lyapunov exponents and parameters regions, have been studied. Moreover, a new DSP system has been designed and implemented for physically realizing various general multiscroll Lorenz attractors.

It should be pointed out that the new approach based on the parameterized *n*th-order polynomial transformation has two prominent features: (a) this approach is self-unified and universal; (b) the system parameters can control bifurcations, maximum Lyapunov exponents, symmetry, and even the shape of the phase portraits of the general multiscroll Lorenz system family.

It should also be emphasized that the DSP-based realization described in this paper provides a feasible way to experimentally generate the complex multiscroll chaotic attractors. Given that it is very difficult to physically realize the complex multiscroll chaotic systems by solving complicated algebraic equations using analog circuit implementations, the proposed DSP-based approach provides a very efficient alternative. Moreover, our numerical simulations and theoretical analysis reveal that the general multiscroll Lorenz system family can easily achieve chaos synchronization, such as complete synchronization and phase synchronization. Therefore, the multiscroll Lorenz system family has alluring prospect in chaos-based information technology, such as secure communications. In particular, comparing with the double-scroll Lorenz system, the general multiscroll Lorenz system family has more scrolls and more complex dynamical behaviors, which nevertheless can be easily controlled by the system parameters. All these characteristics are very useful in many real-world applications.

## ACKNOWLEDGMENTS

This work was supported by the National Natural Science Foundation of China under Grant Nos. 60304017, 20336040, 60221301, and 60572073; the Scientific Research Startup Special Foundation on Excellent Ph.D. Thesis and Presidential Award of the Chinese Academy of Sciences; Natural Science Foundation of Guangdong Province under Grant Nos. 32469 and 5001818; Science and Technology Program of Guangzhou City under Grant No. 2004J1-C0291;

and the Hong Kong Research Grants Council under the CERG Grant CityU 1114/05E.

- <sup>1</sup>E. N. Lorenz, J. Atmos. Sci. **20**, 130 (1963).
- <sup>2</sup>I. Stewart, Nature **406**, 948 (2002).
- <sup>3</sup>G. Chen and T. Ueta, Int. J. Bifurcation Chaos Appl. Sci. Eng. **9**, 1465 (2002).
- <sup>4</sup>A. Vaněček and S. Čelikovský, *Control Systems: From Linear Analysis to Synthesis of Chaos* (Prentice-Hall, London, 1996).
- <sup>5</sup>J. Lü and G. Chen, Int. J. Bifurcation Chaos Appl. Sci. Eng. **12**, 659 (2002).
- <sup>6</sup>J. Lü, G. Chen, D. Cheng, and S. Čelikovský, Int. J. Bifurcation Chaos Appl. Sci. Eng. **12**, 2917 (2002).
- <sup>7</sup>G. Chen and J. Lü, *Dynamics of the Lorenz System Family: Analysis, Control and Synchronization* (Science Press, Beijing, 2003) (in Chinese).
- <sup>8</sup>S. Ozoguz, A. S. Elwakil, and M. P. Kennedy, Int. J. Bifurcation Chaos Appl. Sci. Eng. **12**, 1627 (2002).
- <sup>9</sup>W. Lin and G. Chen, Chaos **16**, 013134 (2006).
- <sup>10</sup>C. Li and G. Chen, Chaos **14**, 343 (2004).
- <sup>11</sup>G. Q. Zhong and K. S. Tang, Int. J. Bifurcation Chaos Appl. Sci. Eng. **12**, 1423 (2002).
- <sup>12</sup>J. Lü, G. Chen, and D. Cheng, Int. J. Bifurcation Chaos Appl. Sci. Eng. **14**, 1507 (2004).
- <sup>13</sup>W. Liu and G. Chen, Int. J. Bifurcation Chaos Appl. Sci. Eng. **13**, 261 (2003).
- <sup>14</sup>A. M. Ruchlidge, J. Fluid Mech. **237**, 209 (1992).
- <sup>15</sup>J. C. Sprott, Phys. Rev. E **50**, R647 (1994).
- <sup>16</sup>J. C. Sprott, Am. J. Phys. **68**, 758 (2000).
- <sup>17</sup>J. C. Sprott, Phys. Lett. A **266**, 19 (2000).
- <sup>18</sup>M. E. Yalcin, J. A. K. Suykens, J. Vandewalle, and S. Ozoguz, Int. J. Bifurcation Chaos Appl. Sci. Eng. **12**, 23 (2002).
- <sup>19</sup>M. E. Yalcin, J. A. K. Suykens, and J. P. L. Vandewalle, *Cellular Neural Networks, Multi-Scroll Chaos and Synchronization* (World Scientific, Singapore, 2005).
- <sup>20</sup>K. S. Tang, G. Q. Zhong, G. Chen, and K. F. Man, IEEE Trans. Circuits Syst., I: Fundam. Theory Appl. **48**, 1369 (2001).
- <sup>21</sup>G. Q. Zhong, K. F. Man, and G. Chen, Int. J. Bifurcation Chaos Appl. Sci. Eng. **12**, 2907 (2002).
- <sup>22</sup>J. Lü, T. Zhou, G. Chen, and X. Yang, Chaos **12**, 344 (2002).
- <sup>23</sup>J. Lü, X. Yu, and G. Chen, IEEE Trans. Circuits Syst., I: Fundam. Theory Appl. **50**, 198 (2003).
- <sup>24</sup>J. Lü, F. Han, X. Yu, and G. Chen, Automatica **40**, 1677 (2004).
- <sup>25</sup>J. Lü, G. Chen, X. Yu, and H. Leung, IEEE Trans. Circuits Syst.-I **51**, 2476 (2004).
- <sup>26</sup>S. M. Yu, J. Lü, H. Leung, and G. Chen, IEEE Trans. Circuits Syst.-I **52**, 1459 (2005).
- <sup>27</sup>J. Lü, S. M. Yu, H. Leung, and G. Chen, IEEE Trans. Circuits Syst.-I **53**, 149 (2006).
- <sup>28</sup>S. M. Yu, S. S. Qiu, and Q. H. Lin, Sci. China, Ser. F **46**, 104 (2003).
- <sup>29</sup>J. Lü and G. Chen, Int. J. Bifurcation Chaos Appl. Sci. Eng. **16**, 775 (2006).
- <sup>30</sup>R. Miranda and E. Stone, Phys. Lett. A **178**, 105 (1993).